THE JOURNAL OF PHYSICAL CHEMISTRY Letters

Letter

pubs.acs.org/JPCL

Photostability of Hydroxocobalamin: Ultrafast Excited State Dynamics and Computational Studies

Theodore E. Wiley,[†] William R. Miller,[†] Nicholas A. Miller,[†] Roseanne J. Sension,*[,†] Piotr Lodowski,[‡] Maria Jaworska,[‡] and Pawel M. Kozlowski*[,§,∥]

[†]Department of Chemistry, University of Michigan, 930 North University Avenue, Ann Arbor, Michigan 48109-1055, United States

[‡]Department of Theoretical Chemistry, Institute of Chemistry, University of Silesia, Szkolna 9, 40-006 Katowice, Poland

[§]Department of Chemistry, University of Louisville, 2320 South Brook Street, Louisville, Kentucky 40292, United States

[∥]Visiting Professor at the Department of Food Sciences, Medical University of Gdansk, Al. Gen. J. Hallera 107, 80-416 Gdansk, Poland

Supporting Information

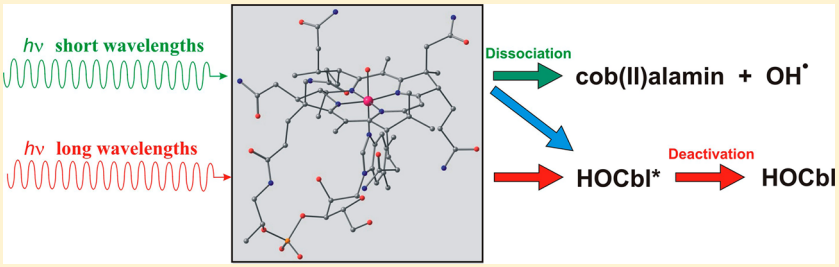

ABSTRACT: Hydroxocobalamin is a potential biocompatible source of photogenerated hydroxyl radicals localized in time and space. The photogeneration of hydroxyl radicals is studied using time-resolved spectroscopy and theoretical simulations. Radicals are only generated for wavelengths <350 nm through a mechanism that involves competition between prompt dissociation and internal conversion. Characterization of the lowest-lying singlet potential energy surface provides insight into the photochemistry of hydroxocobalamin and other cobalamin compounds.

Hydroxocobalamin (HOCbl, Figure 1), a biologically inactive form of vitamin B_{12}, has generated considerable interest since the recent work of Shell and Lawrence, where photolysis of HOCbl in the presence of oxygen was used to cleave plasmid DNA.[1] Application of hydroxyl radicals generated photochemically via homolytic cleavage of the Co−OH offers many advantages in comparison to standard methods, such as the Fenton reaction using Fe^{II} EDTA and H_2O_2. One of the most important advantages to using HOCbl is the possibility of intracellular temporal control by light dependent photoinitiated reactions, in contrast to chemical methods, where initiation and termination of the radical reaction cannot be precisely controlled. However, the mechanism for the photochemical production of hydroxyl radical from HOCbl is unclear. Although alkylcobalamins undergo ready photolysis to produce radicals, nonalkylcobalamins are generally photostable.[2] HOCbl is no exception. Anaerobic photolysis in the presence of a radical scavenger such as sodium benzoate or sorbitol exhibits no measurable photolysis for wavelengths >350 nm. In contrast, photolysis to cob(II)alamin is readily observed following excitation at 253 nm. Photolysis is also observed with a xenon lamp using a pyrex filter to limit the UV, but the rate is ∼2000 times slower than the comparable photolysis of adenosylcobalamin. The threshold

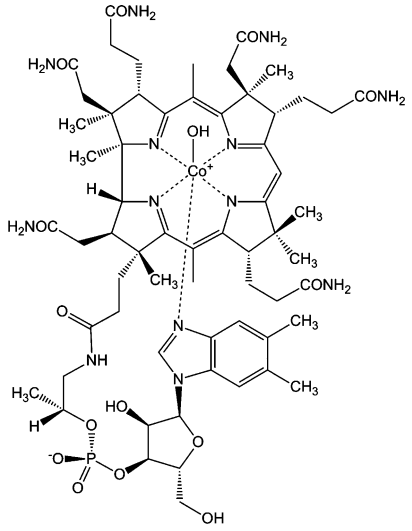

Figure 1. Molecular structure of hydroxocobalamin (HOCbl).

Received: October 19, 2015
Accepted: December 11, 2015
Published: December 11, 2015

DOI: 10.1021/acs.jpclett.5b02333
J. Phys. Chem. Lett. 2016, 7, 143−147

for photolysis falls between 290 and 350 nm. (See Supporting Information Figures S1–S3.)

To explore the mechanism for photochemical production of hydroxyl radicals from HOCbl, broadband femtosecond UV–visible transient absorption spectroscopy was used to characterize the excited electronic states of HOCbl and the results compared with TD-DFT calculations of the potential energy surface of the lowest excited electronic states. An earlier measurement of hydroxocobalamin was performed in D_2O at a pH where the sample was a mixture of DOCbl and D_2OCbl complicating the interpretation.[3] The excited state lifetime of H_2OCbl is substantially shorter than that of HOCbl.[2−4] The sample used here was buffered at pH 10.3 where 99+% of the compound is expected to be HOCbl ($pK_a \sim 8$).[5] The measurements were performed using 404 nm excitation, where no photolysis is expected, and 269 nm excitation, where photolysis to cob(II)alamin is observed in steady state measurements. The probe was a white light continuum (~350 to 800 nm) and (270 to 600 nm) allowing characterization of transient species in the UV–visible region of the spectrum. A typical transient spectrum is plotted in Figure 2.

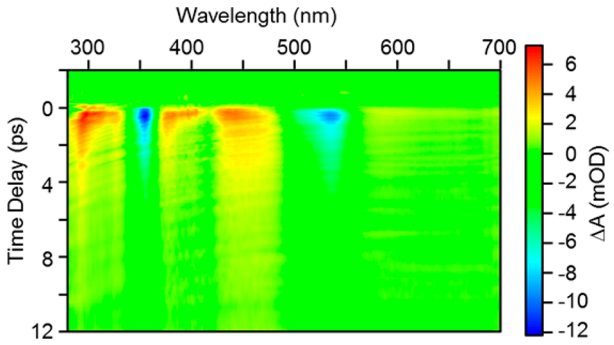

Figure 2. Contour plot of the transient absorption data following excitation at 269 nm. The data obtained following 404 nm excitation are similar (see Supporting Information Figure S4).

The data were fit to a sum of exponentials using a global analysis program.[6] In all cases, the data are well modeled using two exponential decay components: $\tau_1 = 0.32 \pm 0.08$ ps and $\tau_2 = 5.50 \pm 0.17$ ps. There may be a faster component as well, but analysis at short time-delays is complicated by coherent signals from both solvent and solute (see Supporting Information Figures S5–S6 for details of the fits). Typical fits at 540 nm are shown in Figure 3. The difference at early times results from a difference in pulse width and the presence of a strong coherent signal following 404 nm excitation.

Following 404 nm excitation the transient absorption signal decays to baseline. The noise level of the measurement sets an upper limit of <1% on the photolysis yield. Following 269 nm, there is evidence for a photolysis yield of ca. 1.5 ± 0.5% in a persistent, long-lived component that has spectral signatures consistent with cob(II)alamin formation (Figure 3). The steady state photolysis measurements set an upper limit much less than 1% following 404 nm excitation but are consistent with a 1 to 2% yield following 269 nm excitation.

To interpret the transient spectra, we assume a sequential model where excitation produces an excited state, that is, S_n, either directly or following rapid (<100 fs) internal conversion and the S_n state decays to populate the lowest excited singlet state S_1 in 0.32 ± 0.08 ps. The S_1 state decays back to the ground state in 5.50 ± 0.17 ps. The decay associated difference

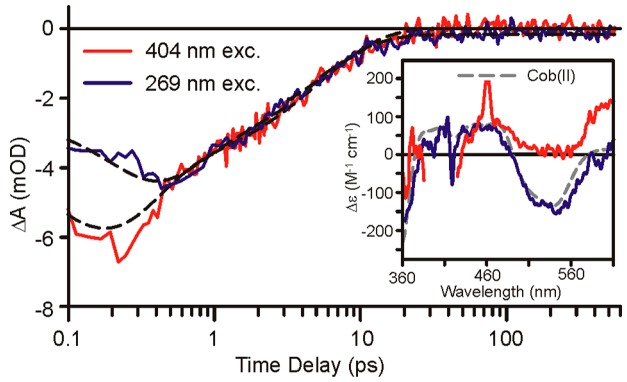

Figure 3. Comparison of time traces at 540 nm following 269 nm excitation and 404 nm excitation. The inset compares the residual difference spectrum at time delays >100 ps with the steady state difference spectrum for photolysis to cob(II)alamin. These data set an upper limit of <1% photolysis yield following 404 nm excitation and 1.5% ± 0.5% photolysis yield following 269 nm excitation.

spectra (DADS) obtained from the amplitudes of the fit to the data can be used to construct the species associated difference spectra (SADS) as described in Supporting Information. The SADS for the S_n and S_1 state are summarized in Figure 4 and

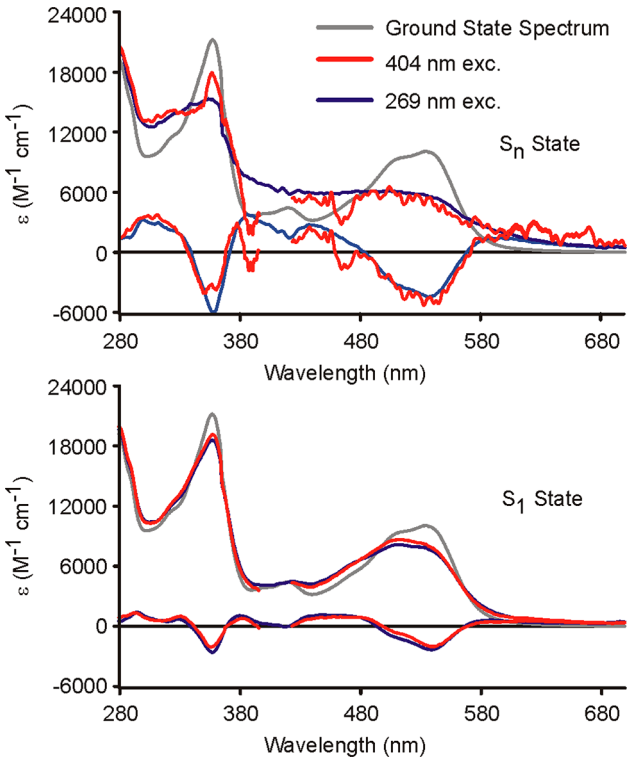

Figure 4. Excited state spectra estimated from the SADS. The excited population is ca. 8% following 404 nm excitation and 13% following 269 nm excitation.

Figure S7 (Supporting Information). The difficulty in separating a coherent component from the S_n contribution following 404 nm excitation results in the larger noise level observed in this SADS.

The SADS can be used to estimate the species associated excited state spectra by adding the appropriate ground state contribution back into the difference spectra: $A(\lambda) = \Delta A(\lambda) + \alpha A_{GS}(\lambda)$ where α is the fraction of the ground state excited by

DOI: 10.1021/acs.jpclett.5b02333
J. Phys. Chem. Lett. 2016, 7, 143–147

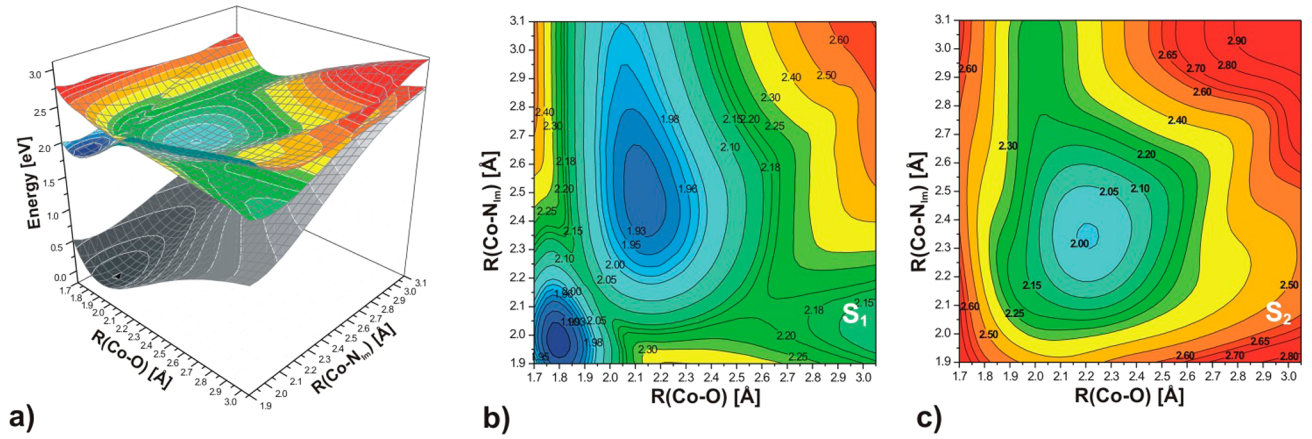

Figure 5. (a) Potential energy surfaces for the ground and two lowest singlet states of the Im−[Co^{III}(corrin)]−OH$^+$ model complex generated as vertical excitations and plotted as a function of axial bond lengths (expressed in angstroms). (b) Vertical projections of the S_1 potential energy surface. (c) Vertical projections of the S_2 potential energy surface.

the pump pulse.[4,7,8] These estimated spectra are placed on an absolute scale using the known extinction coefficients for HOCbl and plotted in Figure 4.

The spectrum of the S_n state is broad, extending across the entire spectral window. The S_1 spectrum is structured, resembling the ground state spectrum. The sensitivity of cobalamin spectra to axial ligation leads to the hypothesis that the S_n state is characterized by significant elongation of the axial bonds, whereas the S_1 state has a structure similar to that of the ground state.[2,8] This is in contrast to the significant displacement observed for the S_1 state of cyanocobalamin.[4,7,8]

To explore the nature of the low-lying excited states of HOCbl, density functional theory (DFT) and time-dependent DFT (TD-DFT) were applied to obtain corresponding potential energy surfaces (PESs). Figure 5 shows these PESs as a function of axial bond lengths. These surfaces were generated using a structural model of HOCbl truncated with respect to side chains (Figure S8 in Supporting Information), employing the BP86/TZVPP level of theory (TZVP basis sets for hydrogen) in all calculations. The energy surfaces corresponding to the lowest excited state (S_1) consists of at least three different electronic states. The involvement of two of them is apparent from the presence of two energy minima, one at shorter Co−OH and Co−N_{Im} distance, and the second at just a slightly elongated Co−OH distance and much longer Co−N_{Im} length. The third state appears on the PES at a Co−OH distance of about 2.5−2.6 Å and within a Co−N_{Im} range of 1.9−2.3 Å, (i.e., the lower right corner of Figure 5b). This part of the S_1 PES has dissociative character consistent with R(Co−OH) energy curves reported previously[9] and involves higher excited states (see also Figure S9 in Supporting Information). Due to the instability of the wave function associated with TD-DFT calculations, this section of the PES cannot be computationally characterized. The minimum of the S_1 state has dominant $p_{OH}/d \rightarrow \pi^*$ character at short Co−OH distance. Upon Co−OH bond elongation, the S_1 state crosses with higher excited states with dominant σ^* contributions and changes character from $p_{OH}/d \rightarrow \pi^*$ to $p_{OH}/d \rightarrow \sigma^*$. For long Co−OH distances, S_1 surface has mainly $p_{OH} \rightarrow \sigma^*$ character with small contribution from d orbital of cobalt.

To obtain a more realistic description of the PES associated with the S_1 state, the geometry of the lowest excited state was optimized as a function of axial bond lengths, for ranges where it was possible (see Supporting Information Figure S10). Overall, the PES corresponding to an adiabatic description of S_1 state does not differ significantly from one generated via vertical excitations. Optimized S_1 axial bond lengths do not differ significantly from those of the ground state as summarized in Figure 6. This is indeed in sharp contrast with CNCbl, where changes are rather significant.[10−13]

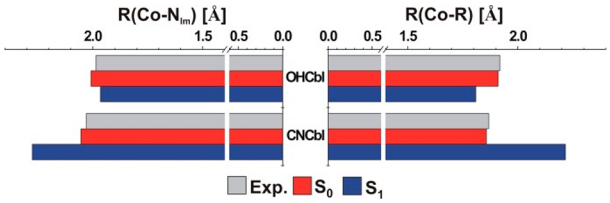

Figure 6. Comparison of Co−R and Co−N_{Im} bond lengths for Im−[Co^{III}(corrin)]−OH$^+$ and Im−[Co^{III}(corrin)]−CN$^+$ model complexes (red, in S_0 optimized geometries; blue, in S_1 optimized geometries; gray, experimental S_0 data[14]).

Closer inspection of the optimized S_1 PES reveals that crossing of the $p_{OH}/d \rightarrow \pi^*$ and $p_{OH}/d \rightarrow \sigma^*$ states takes place when the Co−OH bond length is between 1.85−2.00 Å. The $p_{OH}/d \rightarrow \sigma^*$ state is the same as that obtained from vertical excitations, but with more contribution from cobalt d orbitals. Excited vertical state S_2 about $p_{OH}/d \rightarrow \sigma^*$ character during geometry relaxation lowers in energy and becomes the low-lying S_1 electronic state. In the excited state, the Co−O bond has rather weak bonding character and for stretched Co−OH distances may cross with the ground state (S_0) leading to deactivation. It can be further proposed that the proximity of S_0/S_1 surfaces may lead to deactivation through two possible channels (see Figure S10 in Supporting Information): (a) the first involves elongation and detachment of the axial base followed by corrin ring distortion, (i.e., B($S_{1\ min}$) → C(S_1) → E($S_{1\ min}$) path), a mechanism similar to MeCbl,[15,16] or (b) simultaneous elongation of both axial bonds, (i.e., B($S_{1\ min}$) → C(S_1) → D(S1) path) a mechanism similar to that observed in CNCbl.[13]

The results of femtosecond UV−visible transient absorption spectroscopy, in particular the photostability of HOCbl can be explained assuming the model shown in Figure 7. Because the lowest PES consists of at least three different electronic states (1−3), excitations using longer wavelengths leads effectively to

DOI: 10.1021/acs.jpclett.5b02333
J. Phys. Chem. Lett. 2016, 7, 143−147

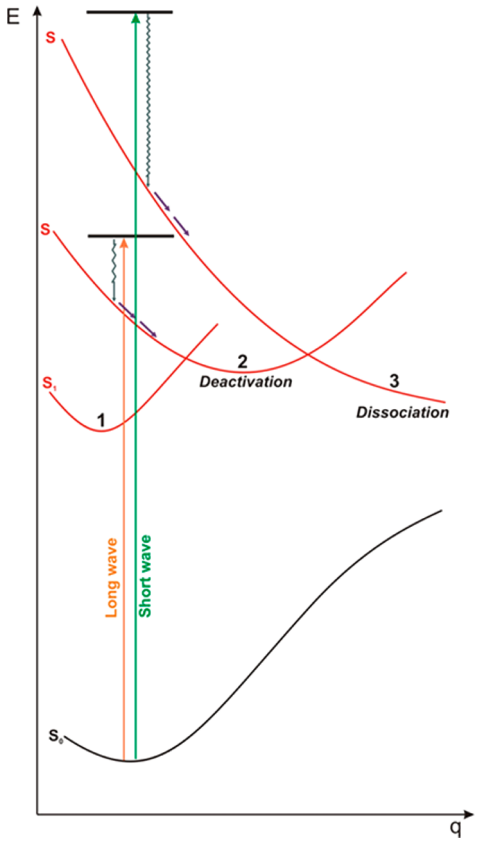

Figure 7. Scheme of potential energy curves involved in in the process of the deactivation and dissociation.

population of the energy minimum corresponding to the $p_{OH}/d \rightarrow \sigma^*$ electronic state (2), which is primarily responsible for deactivation. On the other hand, excitations with shorter wavelengths can populate a repulsive electronic state, with likely dominant $p_{OH}/d \rightarrow \sigma^*$ or $d/p_{OH} \rightarrow \sigma^*$ character, which at longer Co−OH distances becomes dissociative (3).

The comparison of steady state photolysis measurements, transient absorption measurements, and theoretical calculations provide a consistent picture of the photoinduced formation of $OH^{\bullet}$ radicals from HOCbl. The comprehensive picture will help guide the in situ application of HOCbl photolysis as well as the potential photochemical applications of other B_{12} compounds. The relative energies of the three interacting states identified here control the photochemistry and photophysics of many B_{12} compounds and analogs.

■ ASSOCIATED CONTENT

Supporting Information

The Supporting Information is available free of charge on the ACS Publications website at DOI: 10.1021/acs.jpclett.5b02333.

A summary of the steady state photolysis, transient absorption data, fits to the data, potential energy curves and surfaces, along with additional details concerning the calculations and the experimental methods are provided. (PDF)

■ AUTHOR INFORMATION

Corresponding Authors

*E-mail: rsension@umich.edu.
*E-mail: pawel@louisville.edu.

Notes

The authors declare no competing financial interest.

■ ACKNOWLEDGMENTS

The experimental work was supported by grants from the National Science Foundation NSF-CHE 1150660 and NSF-CHE 1464584 to RJS. The theoretical work was supported by the National Science Centre, Poland, under Grant No. UMO-2013/09/B/ST4/03014. The TURBOMOLE calculations were carried out in the Wroclaw Centre for Networking and Supercomputing, WCSS, Wroclaw, Poland, http://www.wcss.wroc.pl, under calculational Grant No. 18 and in the Academic Computer Centre CYFRONET of the University of Science and Technology in Cracow, ACC CYFRONET AGH, Kraków, Poland, http://www.cyfronet.krakow.pl, under Grants MNiSW/SGI3700/USlaski/111/2007 and MNiSW/IBM_BC_HS21/USlaski/111/2007. Visiting professorship of P.M.K. at the Medical University of Gdansk was partially supported by the KNOW program. In addition, P.M.K. would also like to acknowledge the Cardinal Research Cluster (CRC) at the University of Louisville for ensuring exceptional computational resources.

■ REFERENCES

(1) Shell, T. A.; Lawrence, D. S. A New Trick (Hydroxyl Radical Generation) for an Old Vitamin (B_{12}). *J. Am. Chem. Soc.* **2011**, *133*, 2148−2150.
(2) Shiang, J. J.; Cole, A. G.; Sension, R. J.; Hang, K.; Weng, Y.; Trommel, J. S.; Marzilli, L. G.; Lian, T. Ultrafast Excited-State Dynamics in Vitamin B_{12} and Related Cob(III)alamins. *J. Am. Chem. Soc.* **2006**, *128*, 801−808.
(3) Jones, A. R.; Russell, H. J.; Greetham, G. M.; Towrie, M.; Hay, S.; Scrutton, N. S. Ultrafast Infrared Spectral Fingerprints of Vitamin B_{12} and Related Cobalamins. *J. Phys. Chem. A* **2012**, *116*, 5586−5594.
(4) Rury, A. S.; Wiley, T. E.; Sension, R. J. Energy Cascades, Excited State Dynamics, and Photochemistry in Cob(III)alamins and Ferric Porphyrins. *Acc. Chem. Res.* **2015**, *48*, 860−867.
(5) Frey, P. A.; Hegeman, A. *Enzymatic Reaction Mechanisms*; Oxford University Press: New York, 2007; p 191.
(6) Snellenburg, J. J.; Laptenok, S.; Seger, R.; Mullen, K. M.; van Stokkum, I. H. M. Glotaran: A Java-Based Graphical User Interface for the R Package TIMP. *J. Stat. Software* **2012**, *49* (3), 1−22.
(7) Wiley, T. E.; Arruda, B. C.; Miller, N. A.; Lenard, M.; Sension, R. J. Excited Electronic States and Internal Conversion in Cyanocobalamin. *Chin. Chem. Lett.* **2015**, *26*, 439−443.
(8) Harris, D. A.; Stickrath, A. B.; Carroll, E. C.; Sension, R. J. Influence of Environment on the Electronic Structure of Cob(III)-alamins: Time-Resolved Absorption Studies of the S1 State Spectrum and Dynamics. *J. Am. Chem. Soc.* **2007**, *129*, 7578−7585.
(9) Kumar, M.; Kozlowski, P. M. Why Hydroxocobalamin is Photocatalytically Active? *Chem. Phys. Lett.* **2012**, *543*, 133−136.
(10) Lodowski, P.; Jaworska, M.; Kornobis, K.; Andruniow, T.; Kozlowski, P. M. Electronic and Structural Properties of Low-lying Excited States of Vitamin B_{12}. *J. Phys. Chem. B* **2011**, *115*, 13304−13319.
(11) Solheim, H.; Kornobis, K.; Ruud, K.; Kozlowski, P. M. Electronically Excited States of Vitamin B_{12} and Methylcobalamin: Theoretical Analysis of Absorption, CD, and MCD Data. *J. Phys. Chem. B* **2011**, *115*, 737−748.
(12) Kornobis, K.; Kumar, N.; Wong, B. M.; Lodowski, P.; Jaworska, M.; Andruniow, T.; Ruud, K.; Kozlowski, P. M. Electronically Excited States of Vitamin B_{12}: Benchmark Calculations Including Time-Dependent Density Functional Theory and Correlated *ab Initio* Methods. *J. Phys. Chem. A* **2011**, *115*, 1280−1292.
(13) Lodowski, P.; Jaworska, M.; Andruniów, T.; Garabato, B. D.; Kozlowski, P. M. Mechanism of the S_1 Excited State Internal

DOI: 10.1021/acs.jpclett.5b02333
J. Phys. Chem. Lett. 2016, 7, 143−147

Conversion in Vitamin B_{12}. *Phys. Chem. Chem. Phys.* **2014**, *16*, 18675−18679.
(14) Randaccio, L.; Geremia, S.; Nardin, G.; Wuerges, J. X-ray structural chemistry of cobalamins Coord. *Coord. Chem. Rev.* **2006**, *250*, 1332−1350.
(15) Lodowski, P.; Jaworska, M.; Andruniow, T.; Garabato, B. D.; Kozlowski, P. M. Mechanism of Co−C Bond Photolysis in the Base-On Form of Methylcobalamin. *J. Phys. Chem. A* **2014**, *118*, 11718−11734.
(16) Lodowski, P.; Jaworska, M.; Garabato, B. D.; Kozlowski, P. M. Mechanism of Co−C Bond Photolysis in Methylcobalamin: Influence of Axial Base. *J. Phys. Chem. A* **2015**, *119*, 3913−3928.

DOI: 10.1021/acs.jpclett.5b02333
J. Phys. Chem. Lett. 2016, 7, 143−147